LA-UR- 11-04269

Approved for public release; distribution is unlimited.

Title: THE STUDY OF HIGH-SPEED SURFACE DYNAMICS USING A PULSED PROTON BEAM

Author(s): W. T. Buttler, D. M. Oró, D. L. Preston, K. O. Mikaelian, F. J. Cherne, R. S. Hixson, F. G. Mariam, C. Morris, J. B. Stone, G. Terrones and D. Tupa

Intended for: AIP Conference Proceedings on the Shock Compression of Condensed Matter

Los Alamos
NATIONAL LABORATORY
EST. 1943

Los Alamos National Laboratory, an affirmative action/equal opportunity employer, is operated by the Los Alamos National Security, LLC for the National Nuclear Security Administration of the U.S. Department of Energy under contract DE-AC52-06NA25396. By acceptance of this article, the publisher recognizes that the U.S. Government retains a nonexclusive, royalty-free license to publish or reproduce the published form of this contribution, or to allow others to do so, for U.S. Government purposes. Los Alamos National Laboratory requests that the publisher identify this article as work performed under the auspices of the U.S. Department of Energy. Los Alamos National Laboratory strongly supports academic freedom and a researcher's right to publish; as an institution, however, the Laboratory does not endorse the viewpoint of a publication or guarantee its technical correctness.

Form 836 (7/06)

THE STUDY OF HIGH-SPEED SURFACE DYNAMICS USING A PULSED PROTON BEAM

W. T. Buttler*, D. M. Oró*, D. L. Preston†, K. O. Mikaelian, F. J. Cherne‡, R. S. Hixson*, F. G. Mariam*, C. Morris*, J. B. Stone*, G. Terrones§ and D. Tupa***

**Los Alamos National Laboratory, Physics, Los Alamos, NM 87544, USA*
†Los Alamos National Laboratory, X-Computational Physics, Los Alamos, NM 87544, USA
***Lawrence Livermore National Laboratory, Livermore, CA 94551, USA*
‡Los Alamos National Laboratory, Shock & Detonation Physics, Los Alamos, NM 87544, USA
§Los Alamos National Laboratory, X-Theoretical Design, Los Alamos, NM 87544, USA

Abstract. We present experimental results supporting physics based ejecta model development, where we assume ejecta form as a special limiting case of a Richtmyer-Meshkov (RM) instability with Atwood number $A = -1$. We present and use data to test established RM spike and bubble growth rate theory through application of modern laser Doppler velocimetry techniques applied in a novel manner to coincidentally measure bubble and spike velocities from shocked metals. We also explore the link of ejecta formation from a solid material to its plastic flow stress at high-strain rates (10^7/s) and high strains (700%).
Keywords: Ejecta, Ejecta modeling, Richtmyer-Meshkov instability, Proton Radiograhy
PACS: 83.10.Bb, 83.10.Gr, 83.60.Wc

INTRODUCTION

Los Alamos National Laboratory (LANL) is actively engaged in development and implementation of ejecta source and transport models. The effort combines theory with experimental flyer-plate and high-explosive (HE) driven ejecta measurements (see [1, 2, 3]), including measurements presented here from surfaces with larger scale perturbations that permit the study of ejecta physics with dynamic penetrating proton radiography (pRad).

There are at least two approaches to modeling ejecta dynamics. One technique measures total mass-velocity distributions from a variety of surface finishes across a spectrum of shock breakout pressures, P_{SB}. Those source measurements can be inserted into a hydrodynamic-code that adds the measured source into the hydrodynamics when some critical condition is exceeded. Another approach is to characterize materials according to their dynamic material properties and sensitivities to the initial drive conditions. Assuming a robust physics based model can be developed for a spectrum of interesting metals, then the parameter space of variables can be reduced. At a minimum, such a model will accurately predict the total ejected mass and its velocity distribution based on the material and the geometry of the surface perturbations. It is this approach we are pursuing.

THEORETICAL MOTIVATION

We explore ejecta physics around three features: total mass ejected, ejecta mass velocity distributions, and driving conditions under which ejecta do or do not form. The first two criteria link to a liquid RM instability model, while the final criterion links unstable plastic flow to material strength.

Consider the first two criteria, for $A = -1$ for metals that liquefy on shock or shock release, where a shockwave is driven through a metal into sinusoidal perturbations at the metal-vacuum interface. When

the shockwave arrives at the metal-vacuum interface it first releases to zero-pressure at the perturbation minimums and reflects as a rarefaction into the metal. A brief time later the shockwave releases to zero-pressure at the perturbation maximum in the same manner. Under these conditions, strains produced by the shockwave and perturbation interactions causes the perturbation minimums to compress, invert, and then grow in tension as RM instabilities (spikes). The perturbation maximums also invert, forming bubbles that unstably grow into the metal to support spike growth. In this picture, bubbles and spikes refer to peak penetration depths on the two opposite sides of the "free-surface," which we define as the initial zero amplitude of the sinusoidal perturbations, e.g., $\eta(x) = \eta_0 \sin(kx)$, where the wavenumber $k = 2\pi/\lambda$, λ is the wavelength, x is the planar (xz) dimension parallel to the "free-surface" and incident shockwave, and η_0 is the initial perturbation amplitude oriented orthogonal to the xz-plane. In this geometry we take $\eta(x,t)$ positive into the metal, and $-\eta(x,t)$ into the vacuum, and we define $\dot{\eta}^{b,s}(x,t)$ as the velocities of the bubbles (spikes) relative to the free surface velocity u_{fs} – in the laboratory frame we directly measure with laser Doppler velocimetry (LDV, [4]) u_{fs}, $u_b^\infty = u_{fs} - \dot{\eta}^b$, and $u_s^\infty = u_{fs} + |\dot{\eta}^s|$. And we describe the extremely short, early time evolution of the perturbations as they compress during the inversion process with linear theory developed in [5]. For the subsequent period of substantial growth we use a nonlinear model developed in [6].

Setting $g = \eta_0 k = 0$ in Eq. 5a in [6], with some work, permits the approximation of the asymptotic RM spike velocity from Eq. 36 in [7] as $\eta^s \to -\infty$:

$$\lim_{\eta^s \to -\infty} \dot{\eta}(\eta) = \sqrt{3}\dot{\eta}_0^s. \tag{1}$$

This approximation gives the maximum velocity attainable by the spikes in this model.

The approximate bubble velocity is Eq. 17 in [6]

$$\dot{\eta}_t^b = \frac{2\dot{\eta}_0^b}{2 + 3\dot{\eta}_0^b kt} \Longrightarrow \dot{\eta}_\infty^b \equiv \lim_{t\to\infty} \dot{\eta}_t^b = \frac{2}{3kt}. \tag{2}$$

This asymptotic limit applies at very late times and is independent of the initial perturbation amplitudes.

Equations 1 and 2 require the initial growth rates $\dot{\eta}_0^{b,s}$. As shown in [5], for shockwave driven incompressible linear instability growth ($\eta_0 k \ll 1$)

$$\dot{\eta}_0^b = -\dot{\eta}_0^s = \eta_0 k u_{fs}. \tag{3}$$

This result is modified by two effects: compressibility and nonlinearity. For $A = -1$ Meyer and Blewett [8] found the compressibility factor to be:

$$F_{cmp} = 1 - \frac{u_{fs}}{2u_{sh}}, \tag{4}$$

where u_{sh} is the shock velocity in the material at P_{SB}, and for linear amplitudes the bubble and spike compression factors are equivalent: $F_{cmp} \equiv F_{cmp}^{b,s}$.

Reference [9] addresses the nonlinear growth regime through simulations, and [10] provides a nonlinear factor as a fit to the spike simulations in [9]:

$$F_{nl}^s = \frac{1}{1 + (\frac{\eta_0 k}{2})^2}. \tag{5}$$

A fit to the bubble simulations gives a bubble factor:

$$F_{nl}^b = \frac{1}{1 + \frac{\eta_0 k}{6}}. \tag{6}$$

Assuming that the effects of compressibility and nonlinearity act independently we obtain

$$|\dot{\eta}_0^{b,s}| = F_{cmp} F_{nl}^{b,s} |\eta_0 k u_{fs}|. \tag{7}$$

The third criterion evaluates whether ejecta formation is more fundamental than a simple link to the material phase at the time of shock or shock release at the metal-vacuum interface. That is, are the criteria of ejecta formation fundamentally linked to basic material properties? such as material strength at the strains and strain rates in the material as experienced in the interaction of shock induced stresses and the perturbation geometry? If correct ejecta can form when the metal is solid on shock and release. This hypothesis centers on a result in [11] where a model to evaluate the elastic-perfectly plastic yield Y of a material is developed. In [11] they examine unstable growth of perturbations when $A = 1$ (our physics regime is $A = -1$), and they relate Y to spike amplitudes that grow plastically but arrest prior to spike breakup or failure. In Eq. 39 of [11] they find

$$(\xi_m - \xi_0)k \approx 0.29 \frac{\rho(\xi_i k u_p)^2}{Y}, \tag{8}$$

where in our $A = -1$ geometry $\rho \mapsto \rho_0$, $\xi_m \mapsto \eta_\infty^s$, $u_p \mapsto u_{fs}$, and $\xi_0 \approx \eta_0$ when $Y/(\eta_0 k G) \ll 1$, where G is the shear modulus; in practice Y must be the mean flow stress of the material at high strains and high strain rates, and we presume that F_{cmp} and $F_{nl}^{b,s}$ absorb into the scaling parameter, 0.29.

APPROACH, DATA AND DISCUSSION

In designing packages that addressed the full set of needs we settled on use of a P076 driver (76 mm diameter HE lens) and we utilized two different HE boosters: Calcitol for the Sn experiments, and PBX 9501 for the Cu experiment. The final geometries are similar to the design seen in Fig. 1, which incorporates momentum trapping concepts (see [12]).

Figure 2 shows one late time $\times 3$ magnified image from two of three Fig. 1 type pRad experiments: Sn-pRad0425 is to the left (Sn at $P_{SB} = 26.7$ GPa), and Cu-pRad0426 is to the right (Cu at $P_{SB} = 36.1$ GPa). The free-surface velocities u_{fs} were measured with LDV from the flat areas between each perturbation region, and the $\dot{\eta}^{b,s}$ were measured by LDV as well.

When a shocked metal is liquid on shock or release the velocimetry is generally unremarkable. This is observed in liquid release states where the free-surface velocity is seen to jump from zero to u_{fs} and hold steady: it is liquid and retains no significant residual material strength. Because the Sn experiment was shocked to $P_{SB} \gg 19.5$ GPa, the Sn velocimetry falls within this category: an unremarkable result showing only asymptotic bubble, spike, and free-surface velocities – u_b, u_s^∞, and u_{fs} (see [14]). Table 1 shows the liquefied Sn results of interest, such as P_{SB} and the shock velocity u_{sh} at P_{SB} together with $\dot{\eta}_\infty^b$ and $\dot{\eta}_\infty^s$ that are compared with the measured spike and bubble velocities $\dot{\eta}_\infty^{b,m}$ and $\dot{\eta}^{s,m}$. In Table 1 P_{SB} and u_{sh} are estimated from $\langle u_{fs} \rangle$, the average of the three u_{fs} measurements (LDV probes 2, 4, and 6). The $\dot{\eta}^{s,m}$ and $\dot{\eta}^{b,m}$ were coincidentally measured with a single LDV probe above each perturbation region (LDV probes 1, 3, 5, and 7); all measured velocities are known to within 0.01 to 0.02 mm/μs. In the table, the late time measured bubble velocities $\dot{\eta}^{b,m}$ are reported (in a negative sense) relative to $\langle u_{fs} \rangle$. We also report τ_{bo}^s, the time of shock-breakout at the minimum perturbation heights relative to shock breakout at the free-surface, and τ_{rt}^s, the measured time over which the spikes are observed to rise to 90% of their asymptotic velocity $\dot{\eta}_\infty^{s,m}$. The uncertainty in these time values is of $O(0.005\ \mu s)$.

The Cu velocimetry, also presented in Table 1, is more interesting because the Cu remains solid, and it is expected that at least one perturbation region will exhibit unconstrained growth of solid material, one region will exhibit no growth, while at least one region will exhibit growth and arrest. The Cu velocimetry showed that the largest $\eta_0 k = 1.5$ spikes grew unconstrained, the $\eta_0 k = 0.75$ spikes accelerated to a high velocity and then decelerated to a lower asymptotic velocity $u_s^\infty = Const > u_j > u_{fs}^\infty$ (u_j is the maximum measured u_{fs} which is $> u_{fs}^\infty$ of the solid Cu). From the Fig. 2 radiography these $\eta_0 k = 1.5$ and 0.75 spikes also appear to have broken up. The velocimetry in the final two regions shows that the perturbations initially grew but then the spike growth arrested, decaying to $u_\infty^{s,m} = u_{fs}^\infty < u_j$.

Equation 2 implies that the relative difference $|u_{fs}^\infty - \dot{\eta}_\infty^b| \to 0$ at late times, but for liquefied Sn we observe that $\dot{\eta}^b$ is asymptotic and finite by $t \approx 0.3\ \mu s$

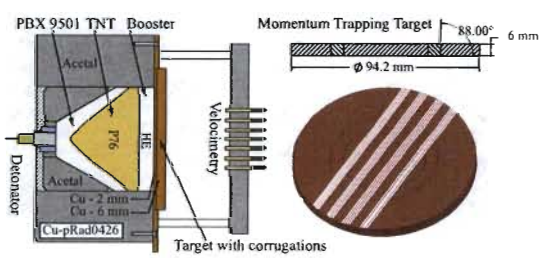

FIGURE 1. pRad RM experimental packages encase a 76 mm diameter plane-wave HE lens in acetal plastic. The lens detonates a HE booster that drives a buffer plate and momentum-trap style target [12] (on right). The targets included four $\lambda = 550\ \mu$m bands of sinusoidal corrugations with varying amplitudes. Each corrugation band was separated by flat regions used to determine velocity histories.

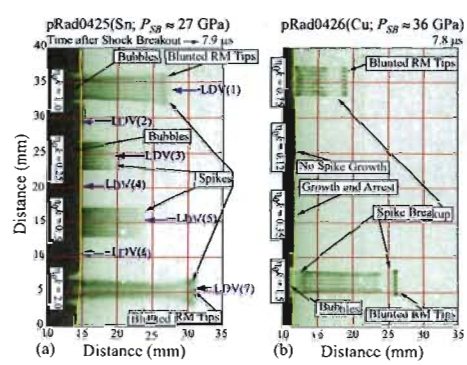

FIGURE 2. Sn (a) and Cu (b) pRad images. The shock-wave breakout is above each image. The perturbation wavelength was $\lambda = 550\ \mu$m; $\eta_0 k$ is shown to the left of each perturbation region; u_{fs} was diagnosed with LDV (a).

TABLE 1. RM instability velocimetry from Sn-pRad0425 and Cu-pRad0426. $\lambda = 0.55$ mm; η_0: initial perturbation amplitude; τ^s_{bo}: time the spikes began to compress and invert from their initial minimums; τ^s_{rt}: time over which the spikes rise to 90% of their maximum velocity; $\dot{\eta}^{b,m}_{t=0.3\ \mu s}$ and $\dot{\eta}^{b}_{t=0.3\ \mu s}$: the measured and predicted bubble velocity relative to u_{fs} at $t = 0.3\ \mu$s; $\dot{\eta}^{s,m}_{\infty}$ and $\dot{\eta}^{s}_{\infty}$: the measured and predicted asymptotic spike velocity; $\dot{\eta}^{s}_{pk}$: the peak measured velocity. The uncertainty in *all* measured velocities is of O(0.01 to 0.02 mm/μs), and the uncertainties in τ^s_{bo} is of O(0.005 μs).

Cu-pRad0426	$\eta_0 k$	η_0 (μm)	τ^s_{bo} (μs)	τ^s_{rt} (μs)	$\dot{\eta}^{b,m}_{t=0.3\ \mu s}$ (mm/μs)	$\dot{\eta}^{b}_{t=0.3\ \mu s}$ (mm/μs)	$\dot{\eta}^{s,m}_{\infty}$ (mm/μs)	$\dot{\eta}^{s}_{pk}$ (mm/μs)	$\dot{\eta}^{s}_{\infty}$ (mm/μs)
$P_{SB} = 36.1$ GPa	0.12	11	≤ 0.00	< 0.08	0.00	N/A	0.00	0.17	0.15
$\langle u_j \rangle \approx 1.58$ (mm/μs)	0.35	31	≤ 0.00	< 0.08	0.00	N/A	0.00	0.57	0.43
$\langle u^{\infty}_{fs} \rangle \approx 1.46$ (mm/μs)	0.75	66	-0.02	< 0.09	-0.02	N/A	0.98	1.30	0.82
$u_{sh} = 5.12$ (mm/μs)	1.5	131	-0.04	?	-0.02	N/A	1.89	1.82	1.20
Sn-pRad0425	0.25	22	-0.01	< 0.14	-0.07	-0.12	0.63	0.63	0.61
$P_{SB} = 26.7$ GPa	0.5	44	-0.02	< 0.13	-0.15	-0.15	1.14	1.14	1.16
$\langle u^{\infty}_{fs} \rangle = 1.85$ (mm/μs)	1.0	88	-0.02	< 0.21	-0.14	-0.17	1.60	1.60	1.97
$u_{sh} = 3.97$ (mm/μs)	2.0	175	-0.09	< 0.34	-0.26	-0.18	2.10	2.10	2.46

to $t > 10\ \mu$s, in contradiction. However the predicted spike velocities were within 20% for the Sn experiment, and the prediction was most consistent for $\eta_0 k < 1$ products that are the most relevant to ejecta production from shocked metals. Unsurprisingly, Eq. 2 does not predict well $\dot{\eta}^b$ for the Cu experiment.

Equation 8 is best exemplified for the Cu $\eta_0 k = 0.35$. For this case the spikes grew from a compressed amplitude of $\approx 27\ \mu$m to $\eta^s \approx 192\ \mu$m, a ratio of 7. The strain rate was $\dot{\varepsilon} > 10^7$/s at zero pressure. It appears the compression factor for $A = 1$ is carried in the Eq. 8 parameter, 0.29, implying it should scale by $[(1 - u_{fs}/(2u_{sh}))/(1 - u_{fs}/u_{sh})]^2 = 1.4$ when $A = -1$, which gives a flow stress of 0.52 GPa. Application of PTW [13] to the $\eta_0 k = 0.35$ Cu gives an average spatial and temporal stress over the spike growth of 0.57 GPa [14].

CONCLUSIONS

Much work remains to be done, the supposition that ejecta form as a limiting case of unstable RM flow is supported. Using such a model we predicted liquid Sn RM spike velocities within 20% of $\dot{\eta}^{s,m}_{\infty}$ for $\eta_0 k \leq 2$. The failure to predict well the bubble velocities is a surprise, but these data present an opportunity to study solid and liquid RM physics of liquid and solid metals in the limit of $A = -1$.

The Eq. 8 RM relation was suggested in [11] for $A = 1$ step-function interface loading pressures. To extract the plastic constitutive properties of real materials from velocimetry data, an analogous relation that includes realistic constitutive relations accounting for work hardening, strain rate sensitivity, and temperature dependence must be derived for $A = -1$.

Special thanks to the pRad core team, G. Dimonte, B. J. Balakumar and (Rusty) T. Gray.

REFERENCES

1. Vogan, W. S., et al., "Piezoelectric characterization of ejecta from shocked tin surfaces," *J. Appl. Phys.* **98**, 113508 (2005).
2. Zellner, M. B., et al., *J. Appl. Phys.* **103**, 123502 (2008).
3. Zellner, M. B. and Buttler, W. T., *Appl. Phys. Lett.* **93**, 114102 (2008).
4. Forman, Jr., J. W., George, E. W. and Lewis, R. D., *Appl. Phys. Lett.* **7**, pp 77-78 (1965).
5. Richtmyer, R. D., *Commun. Pure Appl. Math* **13**, pp 297-319 (1960).
6. Mikaelian, K. O., *Phys. Rev. Lett.* **80**, pp 508-511 (1998).
7. Mikaelian, K. O., *Phys. Rev. E* **81**, 016325 (2010).
8. Meyer, K. A. and Blewett, P. J., *Phys. Fluids* **15**, pp 753-759 (1972).
9. Velikovich, A. L. and Dimonte, G., *Phys. Rev. Lett.* **76**, pp 3112-3115 (1996).
10. Dimonte, G. and Ramaprabhu, R., *Phys. Fluids* **22**, 014104 (2010).
11. Piriz, A. R., Lopez-Cela, J. J., Tahir, N. A., and Hoffmann, D. H. H., *Phys. Rev. E* **78**, 056401 (2008).
12. Bourne, N. K. and Gray, G. T., III, "Computational design of recovery experiments for ductile materials," *Proc. Royal Soc. A* **461**, pp 3297-3313 (2005).
13. Preston, D. L., Tonks, D. L. and Wallace, D. C., *J. Appl. Phys.* **93**, pp 211-220 (2003).
14. Buttler, W. T., et al., "Unstable Richtmyer-Meshkov growth of solid and liquid metals in vacuum," Submitted to *J. Fluid. Mech.* (2011).